Proc. Natl. Acad. Sci. USA
Vol. 75, No. 4, pp. 1938–1942, April 1978
Immunology

RNA content in human lymphocyte subpopulations

(flow cytometry/non-T cells/T cell subpopulations/acridine orange)

M. ANDREEFF, J. D. BECK, Z. DARZYNKIEWICZ, F. TRAGANOS, S. GUPTA, M. R. MELAMED, AND R. A. GOOD

Memorial Sloan-Kettering Cancer Center, New York, New York 10021

Contributed by Robert A. Good, December 12, 1977

ABSTRACT **Human peripheral blood lymphocytes are stained with the metachromatic dye acridine orange and the fluorescence of individual cells is measured by flow cytometry. The relative content of stainable RNA per cell is estimated by comparison with RNase-treated cells. Non-T and T lymphocytes have different mean quantities of RNA per cell, and these classes exhibit different distributions of RNA content. Non-T cells have a unimodal distribution with a sharp peak and exponential distribution towards higher RNA values. T cells have a bimodal distribution with two separate peaks. When T cells having receptors for IgG (T_γ cells) and IgM (T_μ cells) are separated, each of these cell populations displays a unimodal distribution. Of these three lymphocyte subpopulations, T_γ cells have the lowest content of RNA per cell. Non-T cells have slightly higher RNA content than T_γ, and T_μ cells have twice as much RNA as T_γ cells. The RNA content, which surely relates to the different functions of these lymphocyte subpopulations, may also be a useful marker for rapidly distinguishing the lymphocyte subpopulations.**

Although immunologic functions of thymus-derived (T) and bone marrow-derived (B) lymphocytes are very different, their morphologic features are remarkably similar (1, 2). These cell populations are indistinguishable by light microscopy and share a number of cytochemical properties. Differences, however, can be ascertained at the membrane level through analysis of immunologic markers (3, 4). For example, human T lymphocytes consist of at least two subpopulations, namely cells having receptors either for IgG (T_γ) or for IgM (T_μ), as described recently (5, 6). These two subpopulations, although clearly functionally different, have thus far been indistinguishable by morphological and cytochemical criteria.

Applying the recently developed flow cytometric technique for simultaneous staining of cellular DNA and RNA (7, 8) we presently describe differences between non-T and T cells and between T cell subpopulations based on the content of stainable RNA per cell. Flow cytometry, which permits rapid analysis of many cells, makes possible analysis of the variations among cells within subpopulations (9, 10). The present report represents an effort to use this methodology to further characterize the lymphocyte subpopulations.

MATERIALS AND METHODS

Isolation of Lymphocytes. Mononuclear cells (sample I) were separated from 50 cm^3 of heparinized blood of healthy donors by a Ficoll/Hypaque flotation method, as previously described (11, 12). Cells were washed thrice with 0.9% NaCl, resuspended in RPMI-1640 medium (Grand Island Biological Co., Grand Island, NY) containing penicillin (100 units/ml), streptomycin (100 μg/ml), and 20% fetal calf serum, and incubated 30 min at 37° after addition of carbonyl iron particles. Following centrifugation on a Ficoll/Hypaque gradient, density 1.077 g/ml, the cell pellet consisted of monocytes phagocytizing carbonyl iron. The nonphagocytizing cells of the interface were washed thrice in saline (sample II). Fewer than 1% of the cells from the interface were peroxidase positive.

Purification of T Lymphocytes. T lymphocytes were purified from non-T cells by rosetting (one hour, 4°) with sheep erythrocytes and separated on a Ficoll/Hypaque density gradient (30 min, 200 × *g*). The T cells were 90–97% pure as determined by rosette formation with sheep erythrocytes. Cells of this population lacked surface immunoglobulins as ascertained by staining with polyvalent $(Fab')_2$ antiserum to human immunoglobulin (Cappel Laboratories, Cochranville, Pa.). More than 98% of the cells were viable as determined by trypan blue dye exclusion. Non-T cells were removed from the interface of the Ficoll/Hypaque gradient. Sheep erythrocytes attached to T cells were lysed by incubation for 6 min at 37° with Tris buffer containing 0.83% ammonium chloride (sample III). The same incubation was done with non-T cells (sample IV). Cells were then washed thrice in saline.

T Cell Subpopulations. T cells were resuspended in RPMI-1640 medium containing penicillin (100 units/ml), streptomycin (100 μg/ml), and 20% fetal calf serum at a concentration of 2×10^6 cells per ml. These cells were cultured at 37° in a humidified incubator with 5% CO_2/95% air for 20 hr. At the end of the incubation, cells were washed thrice in phosphate-buffered saline and resuspended at a concentration of 4×10^6/ml (sample V). More than 98% of cells were viable as tested by trypan blue dye exclusion. Cells were then assayed for T_μ and T_γ subpopulations as previously described (12).

Antibodies to Ox Erythrocytes. These antibodies were prepared as described elsewhere (13).

Preparation of Ox Erythrocyte–Antibody Complexes. Ox erythrocytes were washed thrice in phosphate-buffered saline and resuspended to a concentration of 2%. Equal volumes of ox erythrocytes and purified rabbit IgM anti-ox erythrocyte antibody (1/250 dilution) or anti-ox IgG antibody (1/100 dilution) were mixed and incubated at room temperature for 90 minutes. Following incubation, cells were washed thrice in phosphate-buffered saline and resuspended to a concentration of 1%. Ox erythrocytes with IgM (EA_m) or IgG (EA_g) were prepared fresh each time.

T Cells with Receptors for IgM (T_μ) and IgG (T_γ). One hundred microliters of EA_m for T_μ or EA_g for T_γ was mixed with 100 μl of T lymphocyte suspension (5×10^6/ml) in 10 different tubes. After centrifugation at 50 × *g* for 5 minutes,

The costs of publication of this article were defrayed in part by the payment of page charges. This article must therefore be hereby marked "*advertisement*" in accordance with 18 U. S. C. §1734 solely to indicate this fact.

Abbreviations: AO, acridine orange; T cells, thymus-dependent lymphocytes; non-T cells; thymus-independent lymphocytes; T_μ, T cells bearing receptors for IgM; T_γ, T cells bearing receptors for IgG; EA, erythrocyte–antibody.

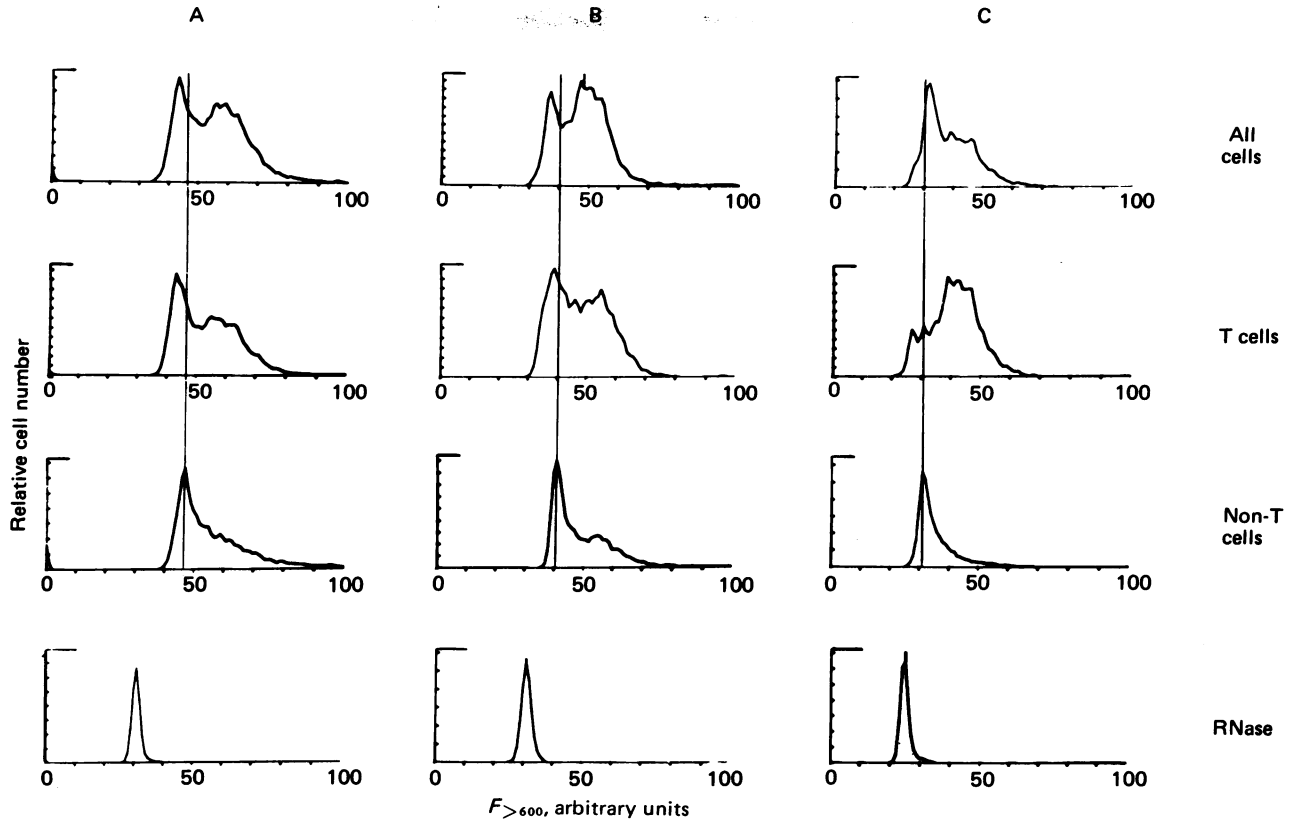

FIG. 1. Computer-drawn histograms representing red fluorescence values ($F_{>600}$) of AO-stained human peripheral blood lymphocytes. Five thousand cells were measured for each histogram. The lymphocytes of three different individuals (*A, B, C*) are presented to illustrate the variation of the RNA distributions between individuals before and after cell separation. Nonseparated mononuclear cells (lymphocytes, after depletion of monocytes, "all cells") show a bimodal distribution with two peaks of various heights. T cells, isolated by rosetting with sheep erythrocytes, also have a bimodal distribution, while non-T cells (predominantly B cells) are characterized by a single peak with an asymmetric distribution skewed towards higher $F_{>600}$ values. For comparison, vertical lines are plotted, indicating positions of B cell peaks in respect to peaks of T cells and nonseparated lymphocytes. B cells have a slightly higher peak value than the first peak of T cells. The lowest row (RNase) indicates $F_{>600}$ of nonseparated lymphocytes following incubation with RNase for 20 min at 37°. The different positions of the peaks among *A, B,* and *C* indicate day-to-day variation of the setting of the flow cytometer; the samples from each individual, however, were measured under identical conditions.

the cells were incubated at 4° for 30 min. Cell pellets from the two incubations were resuspended and centrifuged for 30 minutes at 200 × g in Ficoll/Hypaque gradients. Cells from the interfaces (samples VI, VII) and from the pellets (samples VIII, IX) were collected separately, incubated 6 minutes at 37° in Tris buffer with 0.83% ammonium chloride, and washed thrice in phosphate-buffered 0.9% NaCl. More than 95% of cells were viable as tested by trypan blue dye exclusion.

Staining of DNA and RNA. The method of cell staining is presented in detail elsewhere (8), and was presently used with minor modifications. Aliquots (0.2 ml) of cell suspensions (0.2–0.4 × 10^6 cells) were mixed with 0.4 ml of a solution containing 0.05 M HCl, 0.15 M NaCl, and 0.1% Triton X-100 (Sigma Chemical Corp., St. Louis, MO). After 30 sec, 1.2 ml of a solution containing 0.2 M Na_2HPO_4/0.1 M citric acid buffer (pH 6.0), 1 mM NaEDTA, 0.15 M NaCl, and acridine orange (AO) at 8 μg/ml (AO chromatographically purified, obtained from Polysciences, Inc., Warrington, PA) was added. The cell fluorescence was measured during the next 10 min. As shown before (8), pretreatment of cells with Triton X-100 at low pH makes them permeable to the dye, while nucleic acids remain insoluble in these unfixed cells. Subsequent staining with AO in the presence of chelating agents (EDTA, citrate) results in denaturation of all cellular RNA, which then stains metachromatically red (14) due to electrostatic binding of AO and dye stacking (15), while native DNA intercalates the dye and stains orthochromatically green (16).

The specificity of staining was controlled by incubation of the permeable cells (i.e. after treatment with Triton X-100 and subsequent staining at pH 6.0) with 2 × 10^3 units of RNase per ml, at 37° for 20 min (chromatographically purified RNase, Worthington Biochemical Co., Freehold, NJ), and subsequent measurement under the same conditions, as described (8).

Fluorescence Measurements. Fluorescence of individual cells was measured in the FC 200 Cytofluorograf (Ortho Diagnostic Instruments, Bio/Physics, Westwood, MA) interfaced to a Nova 1220 minicomputer (Data General Corporation, Southboro, MA). Fluorescence and light scatter signals are generated by each cell as it passes through the focus of a 488-nm argon-ion laser beam. The red fluorescence emission ($F_{>600}$, measured in a band from 600 to 650 nm) and the green fluorescence emission (F_{530}, in a band from 515 to 575 nm) from each cell are separated by optical filters and recorded by separate photomultipliers, and the integrated emission values are stored in the computer. Background fluorescence of the AO solution in which cells are suspended is automatically subtracted. The pulse width of green fluorescence, i.e. the time taken by the cell nucleus to pass through the illuminating beam, is also recorded and is used to distinguish single cells from cell doublets, as well as to estimate nuclear size, as described before

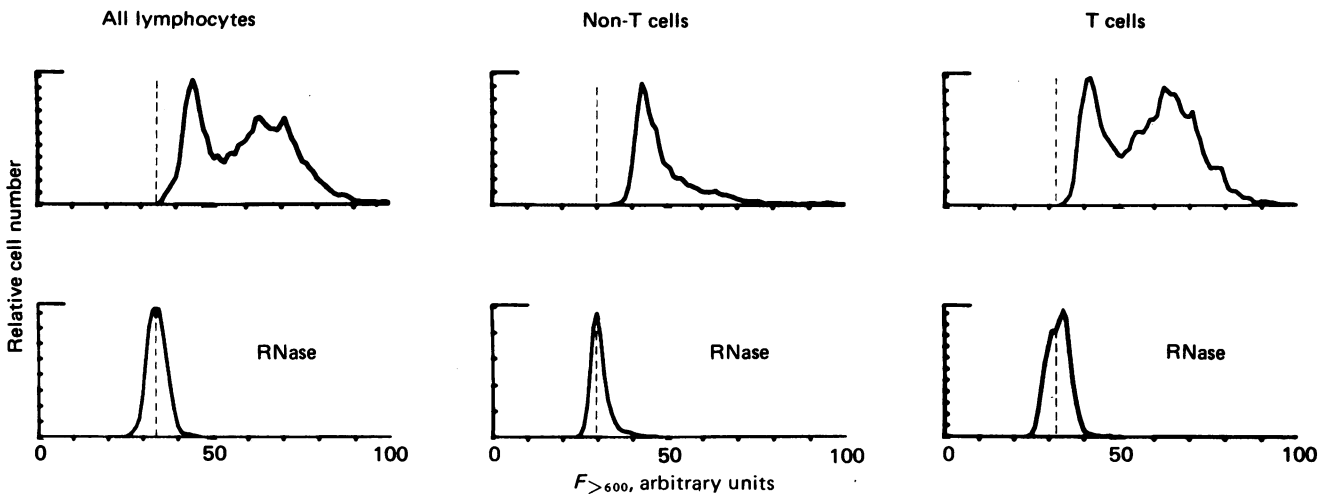

FIG. 2. Computer-drawn histograms displaying red fluoresence ($F_{>600}$) measurements of AO-stained human peripheral blood lymphocytes. The lymphocytes of a single individual were measured under identical conditions: "All lymphocytes" are mononuclear cells after depletion of monocytes (sample II, see *Materials and Methods*), "non-T cells" are nonrosetting (sample IV) lymphocytes, and "T cells" are rosetting (sample III) lymphocytes. The broken lines indicate the mean values of $F_{>600}$ after RNase treatment ($F_{>600}$ unspecific for RNA). These values can be used as a zero point to rescale the ordinate (corrected RNA values, see Table 1). The peak value of non-T cells is slightly higher than that of the first peak of T cells.

(17, 18). More detailed description of the instrument and the computer data-handling system is given elsewhere (9, 17). The data presented are based on a total of 5000 cells measured per sample. The experiment was repeated 10 times on blood from 10 different healthy persons.

Nonstimulated lymphocytes from peripheral blood, when compared with other cell types (i.e., blastoid cells, tissue culture cell lines) have very low quantities of RNA per cell and thus exhibit low intensity of red fluorescence ($F_{>600}$) after AO staining (7). Therefore, the $F_{>600}$ measurements were done in the current experiments at a 10-fold increased $F_{>600}$ photomultiplier sensitivity. Consequently, the nonspecific (RNase-resistant) component of $F_{>600}$ (which presumably reflects some AO stacking on DNA and/or staining of polyanions other than RNA) is relatively high. The RNase-sensitive component of $F_{>600}$, in contrast to other cell types in which it represents over 85% of the total $F_{>600}$ (7), is only 30–60% of the total $F_{>600}$ in lymphocytes (see figures and tables). In all of the data presented, therefore, the control measurements of the RNase-treated cells are included, to indicate the quantity of stainable RNA in relation to total $F_{>600}$.

RESULTS

DNA Distribution. The DNA of the total lymphocytes and the several subpopulations as measured by AO green fluorescence displays a unimodal distribution around the G_0/G_1 peak, fewer than 1% of the cells being in the S phase of the cell cycle. The coefficient of variation of the mean value of the measurements was between 3% and 4%, and no difference in the mean values was detected (data not shown).

RNA Distribution. Frequency histograms of RNA content of the nonseparated lymphocytes show a bimodal distribution indicating the presence of at least two cell subpopulations with different RNA contents (Fig. 1, upper row). Large differences were observed among normal individuals, expressed as variations in the respective heights of the peaks. The variations observed from person to person are illustrated in Fig. 1, which shows representative samples from three individuals. Measurements of isolated T cells (sample III; Fig. 1, second row) also display a bimodal distribution, while non-T cells (predominantly B cells, sample IV) have a unimodal distribution with a low value, a sharp peak, and an exponential shape towards higher values (Fig. 1, third row). In this respect, the shape of the non-T cell RNA histograms is uniform in samples from all individuals. In all samples the non-T cells have higher $F_{>600}$ values than the median of the first T-cell peak, as indicated by the vertical line in Fig. 1.

The bimodal shape of RNA histograms of T cells indicates at least two T cell subpopulations (Fig. 1 and 2). When T_γ and T_μ cell subpopulations are separated (Fig. 3) and measured, each displays a unimodal RNA distribution. Thus, T_γ cells have a peak value at low fluorescence intensity skewed to the right; T_μ cells, on the other hand, have higher fluorescence and the distribution is skewed to the left.

The cells found in the interfaces of T_γ and T_μ gradients show, as expected, complementary distributions of RNA as compared to those cells found in the pellets, indicating the presence of T_μ cells in the interface of the T_γ gradient and vice versa.

The histograms shown in Fig. 2 and 3 are all from the same experiment; their numerical evaluations are presented in Tables 1 and 2. In Table 1, after subtraction of nonspecific red fluorescence, corrected RNA values describe the sequence of the three peaks ($T_{peak\ 1}$, non-T, $T_{peak\ 2}$) according to their increasing RNA content. $T_{peak\ 2}$ has more than twice the RNA content of $T_{peak\ 1}$; non-T is slightly higher than $T_{peak\ 1}$. Table 2 (corresponding to Fig. 3) shows values of T cells incubated for 20 hr and of separated T_γ and T_μ cells. Again, the corrected peak value of T_μ cells is more than twice as high as that of the T_γ cells. The coefficient of variation of the mean values of these measurements was between 9% and 20%. Because of the skewness of the distributions (which might be related to incomplete separation of the subpopulations) the peak values are more descriptive than the mean values.

Nuclear Diameter. Measurements of nuclear diameter by use of the green pulse width show small but consistent differences in all experiments between T (mean value 37.8) and non-T (mean value 39.1) cells (Table 1). No difference, however, is found between T_μ and T_γ cells (Table 2). The coefficient of variation of these measurements is 4–6%.

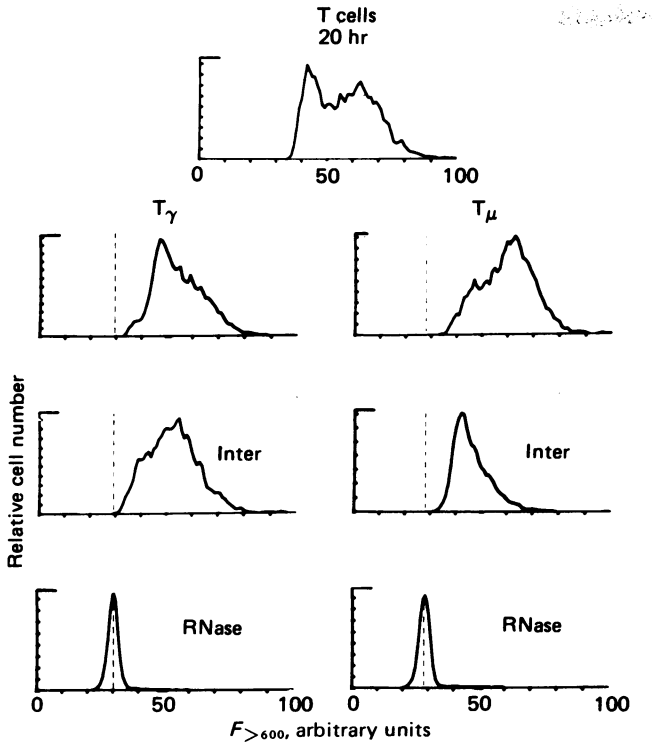

FIG. 3. Computer-drawn histograms displaying red fluorescence ($F_{>600}$) of AO-stained human peripheral blood T lymphocytes. Separated T cells (histogram shown in Fig. 2) were incubated in RPMI-1640 medium supplemented with 20% fetal calf serum at 37° for 20 hr ("T cells 20 hr"; see *Materials and Methods*, sample V). The bimodal distribution of these cells is still apparent following incubation. Incubation of these cells with ox erythrocytes coated with either IgM or IgG results in rosette formation. Rosetting cells were separated from nonrosetting cells by Ficoll/Hypaque gradient centrifugation. Rosetting cells, found in the pellet, were either T_μ or T_γ. Their $F_{>600}$ histograms are unimodal and skewed either to the right (T_γ) or to the left (T_μ). Cells found in the interfaces of the gradients ("Inter") display reversed $F_{>600}$ distributions (see text). Incubation of T_μ and T_γ cells with RNase results in narrowly distributed histograms with lower peak values, as shown in the bottom row. The broken lines can be used to rescale the ordinate. For numerical evaluation see Table 2.

DISCUSSION

The lymphocyte populations have been subdivided in both human and animal systems according to their immunological functions. While B lymphocytes produce antibodies (1, 4), the T lymphocytes are responsible for cell-mediated immunity. T_γ cells act as suppressor cells and T_μ cells as "helper" cells in the differentiation of B cells (19). T_μ and T_γ have been observed to differ in their sensitivities to prednisolone, ionizing radiation, and influences by thymopoietin (13). They also manifest different dose–response patterns to phytohemagglutinin and vary in relative proportions in patients with immunodeficiencies (6, 12). Receptors for IgM and IgG were found on leukemic blast cells with T cell properties (E rosettes) (20).

In the present study, several subpopulations of lymphocytes have been shown to vary in the amount of AO-stainable RNA. Because it may be assumed that different cell functions require different proteins, which implies differences in transcriptional and translational activities, it should not be surprising to find various quantities and intercellular distributions of RNA in the several functionally identifiable lymphocyte subpopulations. It has been shown by use of metabolic inhibitors that formation of rosettes with sheep erythrocytes requires transcription, translation, and protein synthesis (21).

Table 1. Fluorescence values of acridine orange-stained T and non-T lymphocytes

		All lympho-cytes	Non-T cells	T cells		
				Peak 1	Total	Peak 2
AO	Mean	59.7	50.2	43.3	58.0	65.7
	Peak	45	43	41	41	63
AO + RNase	Mean	34.2	30.8		32.9	
	Peak	35	30		34	
$F_{>600}$, % loss	Mean	42.7	38.6	24.0	43.2	49.9
	Peak	22.7	30.2	17.1	17.1	46.0
Corrected value	Mean	25.5	19.4	10.4	25.1	32.8
	Peak	10	13	8	8	19
Green pulse width	Mean		39.1		37.8	

Red fluorescence ($F_{>600}$) peak and mean values of human peripheral blood lymphocytes stained with AO. The AO row = $F_{>600}$ after staining with AO as described in *Materials and Methods*; AO + RNase = $F_{>600}$ after treatment with RNase; $F_{>600}$, % loss = decrease of $F_{>600}$ after treatment with RNase in percent as compared to AO; corrected value = relative $F_{>600}$ values in arbitrary units, given as differences between AO and AO + RNase; green pulse width = measure of nuclear diameter in arbitrary units. All lymphocytes = lymphocytes prepared as described in *Materials and Methods*, sample II; non-T = nonrosetting cells (predominantly B cells); T cells = cells forming rosettes with sheep erythrocytes.

Non-T cells display a unimodal, exponential distribution of RNA with a relatively low mean value. The non-T lymphocytes with higher amounts of RNA probably represent cells responding to antigens; e.g., lymphocytes respond to antigenic stimuli with an increase in cellular RNA content prior to DNA synthesis (7). Interestingly, the shape of the distribution of non-T cells according to their RNA content is strikingly similar to that reflecting esterase activity in these cells (ref. 22; tentatively confirmed in our laboratory). This curve is also similar to that defining the distribution of cells engaged in antibody production (23).

The bimodal distribution of T cells appears to be a consequence of the presence of two subpopulations of lymphocytes that have different RNA contents. The mean RNA content of T_γ lymphocytes is slightly lower than that of non-T cells. T_μ

Table 2. Fluorescence values of acridine-orange stained T cell subpopulations

		T (20 hr)	T_γ	T_μ
AO	Mean	56.7	54.5	59.7
	Peak	42	47	63
AO + RNase	Mean	—	30.6	29.3
	Peak	—	31	29
$F_{>600}$, % loss	Mean	—	43.9	50.9
	Peak	—	34	54
Corrected value	Mean	—	23.9	30.4
	Peak	—	16	34
Green pulse width	Mean	37.8	37.8	37.7

Red fluorescence ($F_{>600}$) peak and mean values of human peripheral blood T lymphocytes and T lymphocyte subpopulations stained with AO. Abbreviations are as described for Table 1. T (20 hr) = T cells incubated in RPMI-1640 medium for 20 hr. For details of preparation see text.

lymphocytes, on the other hand, have a higher RNA content than non-T cells and twice the RNA content of T_γ cells. The non-gaussian distribution of RNA content in both T_μ and T_γ cells may be the consequence of either incomplete separation of two populations by the rosette technique employed or the existence of different functional states within each subpopulation. Alternatively, this finding might reflect the existence of additional T cell subpopulations not yet identified.

Since biochemical evidence suggests that about 80% of the total RNA in each of the cell types is composed of rRNA (24), it appears the present method reveals mostly rRNA, and the total amount of tRNA, heterogeneous nuclear RNA, and mRNA cannot be larger than 20% (14). It should be emphasized that the *content* of RNA, as presently detected, may not necessarily be directly correlated with the rate of RNA *synthesis*, i.e., revealed by [^{3}H]uridine incorporation. The content is a function of the rates of both RNA synthesis and RNA degradation. It is entirely possible that the turnover of RNA varies in lymphocyte subpopulations.

A second parameter, nuclear diameter, also appears to differ between non-T and T cells. Estimation of nuclear size, which can be derived from the green fluorescence pulse width measurement, revealed that non-T cell nuclei are larger than T cell nuclei, but no differences were observed between the sizes of T_μ and T_γ cell nuclei.

The results described herein show that lymphocyte subpopulations can be identified by a metabolic marker, namely by RNA content. This nonimmunological parameter certainly relates to the immunological functions of these cells and provides, in addition, a new marker for identifying the lymphocyte subpopulations. This marker alone, while it can serve to separate T cell subpopulations, is not adequate to distinguish between T_γ and non-T cells. Because T and non-T cell subpopulations are distinguishable by their esterase activity (22), the combination of these two methods, both of which can be quantified by flow cytometry, should provide a method for separating and analyzing these three lymphocyte subpopulations.

The authors wish to thank Miss R. Nager for her assistance in the preparation of this manuscript and Mr. L. J. Nelson for his expert technical assistance in the separation of lymphocyte subpopulations. This research was supported by Deutsche Forschungsgemeinschaft Grants An 109/2 and Be 728/1; National Institutes of Health Grants 2 R 26 CA 14134, CA-08748, CA-19267, AI-11843, and NS-11457; and the Judith Harris Selig Memorial Fund.

1. McConnell, I. (1975) in *The Immune System*, eds. Hobart, M. J. & McConnell, I. (Blackwell, Oxford, England), pp. 98–119.
2. Fischer, K., Cohnen, G., Szaniawski, W. & Brittinger, G. (1977) *Acta Haematol.* **57**, 247–256.
3. Aiuti, F., Cerottini, J. C., Coombs, R. R. A., Cooper, M. & Dickler, H. B. (1973) *Scand. J. Immunol.* **3**, 521–532.
4. Bentwich, Z. & Kunkel, H. G. (1973) *Transplant. Rev.* **16**, 29–50.
5. Moretta, L., Ferrarini, M., Durante, L. & Mingari, M. C. (1975) *Eur. J. Immunol.* **5**, 565.
6. Moretta, L., Ferrarini, M., Mingari, M. C., Moretta, A. & Webb, S. R. (1976) *J. Immunol.* **117**, 2171–2180.
7. Darzynkiewicz, Z., Traganos, F., Sharpless, T. & Melamed, M. R. (1976) *Proc. Natl. Acad. Sci. USA* **73**, 2881–2884.
8. Traganos, F., Darzynkiewicz, Z., Sharpless, T. & Melamed, M. R. (1977) *J. Histochem. Cytochem.* **25**, 46–56.
9. Melamed, M. R., Darzynkiewicz, Z., Traganos, F. & Sharpless, T. (1977) *Cancer Res.* **37**, 2806–2812.
10. Andreeff, M. (1977) *Zellkinetik des Tumorwachstums. Grundlagen-Methoden-Experimente* (G. Thieme Verlag, Stuttgart, Germany).
11. Bøyum, A. (1977) *Lymphology* **10**, 71–76.
12. Gupta, S. & Good, R. A. (1977) *Clin. Exp. Immunol.*, **30**, 222.
13. Gupta, S. & Good, R. A. (1977) *Cell. Immunol.* **34**, 10–18.
14. Darzynkiewicz, Z., Traganos, F., Sharpless, T. & Melamed, M. R. (1975) *Exp. Cell Res.* **95**, 143–155.
15. Bradley, D. R. & Wolf, M. K. (1959) *Proc. Natl. Acad. Sci. USA* **45**, 944–952.
16. Lerman, L. S. (1963) *Proc. Natl. Acad. Sci. USA* **49**, 94–102.
17. Sharpless, T., Traganos, F., Darzynkiewicz, Z. & Melamed, M. R. (1975) *Acta Cytol.* **19**, 577–581.
18. Sharpless, T. K. & Melamed, M. R. (1976) *J. Histochem. Cytochem.* **24**, 257–264.
19. Moretta, L., Webb, S. R., Grossi, C. E., Lydyard, P. M. & Cooper, M. D. (1977) *J. Exp. Med.* **146**, 189.
20. Moretta, L., Mingari, M. C., Moretta, A. & Lydyard, P. M. (1977) *Clin. Immunol. Immunopathol.* **7**, 405–409.
21. Bushkin, S., Pantic, V. S. & Good, R. A. (1975) *J. Immunol.* **115**, 866–870.
22. Wilder, M. E. & Cram, L. S. (1977) *J. Histochem. Cytochem.* **25**, 888–891.
23. Loken, M. R., Parks, D. R. & Herzenberg, L. A. (1977) *J. Histochem. Cytochem.* **25**, 899–907.
24. Davidson, J. N. (1972) *The Biochemistry of Nucleic Acids* (Academic, New York), p.76.